Computational Energy Science

Vol. 1, No. 3, p. 138-149, 2024

Original article

A new mathematical model of pressure buildup analysis for a well produced at constant bottomhole pressure

Jing Lu[1]*, Qing Nie[1], Erlong Yang[1]*

[1]Key Lab of Enhanced Oil Recovery, Ministry of Education, Northeast Petroleum University, Heilong Jiang 163000, P. R. China

Keywords:
Mathematical model
pressure buildup
constant bottomhole pressure

Cited as:
Lu, J., Nie, Q., Yang, E. A new mathematical model of pressure buildup analysis for a well produced at constant bottomhole pressure. Computational Energy Science, 2024, 1(3): 138-149.
https://doi.org/10.46690/compes.2024.03.02

Abstract:
This paper presents a computationally efficient and convenient method with simple procedures to forecast the pressure buildup if a well produced at constant bottomhole pressure prior to shut-in in a closed rectangular-shaped reservoir. The proposed algorithm is based on an analytical model with numerical approximation, and the pressure buildup is predicted through a series of mathematical methods such as the Laplace transform, the Green's function and the superposition principle. The proposed model is validated by the Computer Modeling Group (CMG) simulation, the results show that the proposed model is accurate enough to predict the pressure buildup behavior of a well produced at constant bottomhole pressure prior to shut-in in a closed rectangular reservoir. The conventional models presented in the literature are mostly empirical or semi-analytical, which are not grounded in fundamental theory. Our proposed model has a solid theoretical basis, it provides a computationally efficient and convenient method for predicting pressure buildup behavior of a well produced at constant bottomhole pressure prior to shut-in in a closed rectangular reservoir. We conclude that the reservoir boundary condition, the reservoir size, the well location, the production pressure difference and the well production time prior to shut-in have significant effects on the pressure buildup behavior.

1. Introduction

When a flowing well is shut in, the pressure in the wellbore increases with time as the pressures throughout the reservoir approach a static value. Analysis of pressure buildup after a well is shut in often provides critical information about the reservoir and well. One of the most important aspects of formation evaluation is the design, implementation, and interpretation of a pressure buildup test. Basically, this test requires that a producing well be shut in and that the associated change in bottomhole pressure be measured as a function of shut-in time.

Theis (1935) showed that buildup pressures in a shut-in water well should be a linear function of the logarithm of the time ratio $(t+D_t)/D_t$. Muskat (1937) discussed pressure buildup in oil wells and proposed determination of static pressure by a semi-log trial-and-error plot that has been found to be applicable to a variety of buildup cases. Van Everdingen and Hurst (1949) revived interest in transient pressure analysis with their paper on the behavior of unsteady-state fluid flow in a porous media. Miller et al (1950) presented an analysis for buildup when the well had been produced long enough to reach pseudo steady state prior to shut-in. Their work indicated that buildup pressures should plot as a linear function of the logarithm of shut-in time. Horner (1951) presented a study of pressure buildup semi-log curve identical with the Theis curve and recommended a method for extrapolation to fully build up static pressure for a closed circular reservoir. This sort of semi-log pressure buildup plot is often referred to as a Horner plot in the oil industry. As in the Horner plot, the slope of the straight line is inversely proportional to the mean formation effective permeability. Both Horner and Miller-Dyes-Hutchinson had presented methods for determining permeability and static pressure from buildup data.

Significantly, the Homer technique was developed for the buildup case of a constant production-rate well located in an infinitely large reservoir. The MDH method was developed for the case of a well located in the center of a closed (no-flow

*Corresponding author.
E-mail address: nepulj@nepu.edu.cn (J. Lu); 871789003@qq.com (Q. Nie); yangerlong@nepu.edu.cn (E. Yang).

Received July 10, 2024; revised August 16, 2024; accepted September 16, 2024; available online September 19, 2024.

outer boundary) circular reservoir and produced to pseudo-steady state before shut in.

The concept of formation damage, or skin factor, was introduced to transient pressure analysis by Van Everdingen (1953) and Hurst (1953). They discussed its effect on well behavior and presented methods for evaluating its presence. Probably the most reliable estimate of the skin factor is obtained from a pressure-buildup test. Specifically, the evaluation method makes use of the slope of the Horner or MDH semi-log straight line.

Matthews et al (1954) extended Horner's determination of static pressure for bounded circular reservoirs to the general case of a well in almost any position within a large variety of bounded drainage shapes. Matthews (1961) studied pressure buildup curve to show how reservoir properties and fluid properties and wellbore conditions tend to distort the idealized picture. Dietz (1965) proposed a method to determine average reservoir pressure from pressure buildup data. Ramey and Cobb (1971) presented a general pressure buildup theory for a well produced at a constant flow rate before shut-in in a closed drainage area.

Kazemi (1974) presented two simple and equivalent procedures for improving the calculated average reservoir pressure buildup tests in developed reservoirs. Cobb and Smith (1974) generated pressure buildup data further for a variety of well locations within various rectangular drainage shapes and studied the resulting curves for diagnostic features and rules. Chen and Brigham (1978) investigated the effect of wellbore storage and skin on pressure buildup behavior. Guppy et al (1982) presented pressure buildup analysis of fractured wells producing at high flow rates. Streltsova (1984) presented pressure buildup analysis for interference tests in stratified formations. Olarewaju and Lee (1989) presented a study of pressure buildup behavior of partially completed wells in layered reservoirs. Bossie-Codreanu (1989) presented a method to determine drainage area of wells that were shut in after having reached pseudo-steady state flow conditions. Onur et al (1991) investigated the buildup response of a well located in a system of producing wells completed in a closed, bounded reservoir, assuming that pseudo-steady state had been reached at the instant of shut-in. Umnuayponwiwat and Ozkan (2000) investigated the effect of interference between neighboring wells during buildup analysis for wells producing at different constant flow rates in a multi-well system. Lin and Yang (2005) presented a method for analyzing pressure buildup data from a well located in a system with both production and injection wells at constant rates in a closed, two-phase flow reservoir. Deng et al (2015) presented a method for analyzing pressure buildup data from a well located in a multiwell reservoir, assuming that the testing well and adjoining wells being shut in at the same time.

The above conventional models presented in the literature were developed for wells either at a constant surface rate or at a series of discrete constant rates prior to shut-in. As a matter of fact, constant bottomhole pressure production are not uncommon. Conditions under which constant pressure is maintained include steam production into a back-pressured turbine, production in a tight reservoir or open flow to the atmosphere.

There are, in the petroleum literature, several papers addressed problems concerning buildup analysis of wells produced at constant bottomhole pressures before shut-in. Clegg (1967) used the Laplace transform to obtain an approximate buildup solution after large producing times, and he used conventional semi-log techniques. Uraiet and Raghavan (1980) used finite difference method for pressure buildup of a well located at the center of a circular drainage area and produced at constant bottomhole pressure. Ehlig-Economides and Ramey (1981) used the method of superposition in time of continuously changing flow rates prior to shut-in to generate a solution for pressure buildup following constant pressure flow. Ohaeri (1983) presented pressure buildup analysis for a well produced at constant pressure in a naturally fractured reservoir. Kutasov (1989) presented an analytical solution to describe the pressure buildup for wells produced at constant bottomhole pressures in an infinite-acting reservoir. Camacho-V et al. (2002) presented an analytical solution to obtain the shut-in bottomhole pressure at a vertical well that had been producing at a constant wellbore pressure from a closed boundary reservoir with multiple wells producing at constant, but different wellbore pressures. Lu at al (2018) proposed an algorithm to calculate buildup pressure of a well produced at constant bottomhole pressure prior to shut-in in an infinite reservoir. Prats et al (2020) obtained analytic expressions of buildup pressure resulting from shutting in a well after producing it at constant pressure, in both Laplace space and time, but their proposed algorithm was tedious and cumbersome.

However, the models presented in the literature of pressure buildup analysis for a well produced at constant pressure prior to shut-in are mostly empirical, which are not grounded in fundamental theory. And the analysis procedures in the literature are tedious and cumbersome. Hence, there is a need for a thorough treatment of pressure buildup behavior following constant-pressure production.

This paper presents a computationally efficient and convenient method with simple procedures to forecast the pressure buildup if a well produced at constant bottomhole pressure prior to shut-in in a closed rectangular-shaped reservoir. The effects of the reservoir boundary condition, the reservoir size, the well location and the production pressure difference on the pressure buildup behavior are studied.

2. Analytical model

2.1 Basic assumptions

The basic assumptions are shown as follows:

- The reservoir has a closed boxed drainage domain with constant thickness, porosity, and permeability. Also the porous volume is bounded by lateral, top, and bottom closed boundaries.
- Initially, the reservoir has constant pressure and it is above the bubble point pressure during the field life. The transient pressure has transmitted to lateral reservoir boundary.
- One well is arbitrarily located in the box-shaped reservoir, and the well is produced at constant bottomhole pressure

prior to shut-in.

- The fluid is a single-phase liquid, with slight compressibility, constant viscosity, and formation volume factor. Also, we neglect the effect of pressure on fluid properties and gravity forces.

2.2 Governing equation, initial and boundary conditions.

The reservoir domain is a rectangular parallelepiped with length a, width b and height h, which can be expressed below:

$$\Omega = (0,a) \times (0,b) \times (0,h) \tag{1}$$

The production well is a fully penetrating vertical well, thus we may investigate the production performance in two-dimensional space, i.e. the well is in a rectangular-shaped reservoir. We assume the lower left point of the rectangular is the origin point of the Cartesian coordinate system, the well is located at (x_w, y_w), as shown in Fig. 1. And the well is produced at constant flowing bottomhole pressure, P_w.

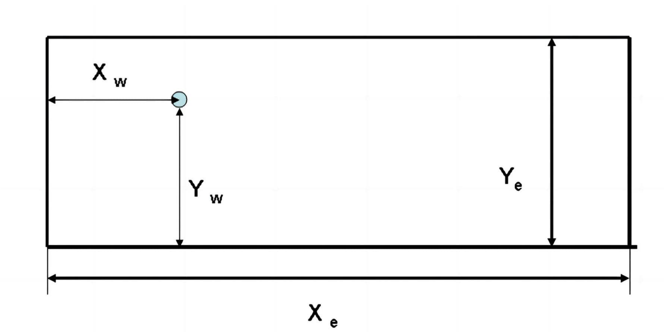

Fig. 1. One well in rectangular-shaped reservoir.

We can obtain the governing equation for one well in a rectangular-shaped reservoir (Lee et al, 2003; Lu et al, 2019):

$$\frac{\partial^2 P}{\partial x^2} + \frac{\partial^2 P}{\partial y^2} = \left(\frac{\phi \mu C_t}{K}\right)\frac{\partial P}{\partial t} + \left(\frac{\mu B}{Kh}\right) q(t)\delta(x-x_w)\delta(y-y_w) \tag{2}$$

where P is pressure in the reservoir, $q(t)$ is the transient flow rate of the well, ϕ is porosity, μ is viscosity, h is payzone thickness, K is permeability, C_t is the total reservoir compressibility, B is formation volume factor.

Note that, the reservoir has constant initial pressure everywhere:

$$P(t,x,y)|_{t=0} = P_{ini} \tag{3}$$

All the reservoir boundaries are impermeable:

$$\frac{\partial P}{\partial x}|_{x=0,a} = \frac{\partial P}{\partial y}|_{y=0,b} = \frac{\partial P}{\partial z}|_{z=0,h} = 0 \tag{4}$$

The well is produced at constant flowing bottomhole pressure:

$$P(t,x_w,y_w) = P_w \tag{5}$$

2.3 Dimensionless transformation

To simplify the governing equation, we define the following dimensionless groups (Lu at al, 2018):

$$x_D = \frac{x}{h}, y_D = \frac{y}{h}, r_{wD} = \frac{a}{h}, a_D = \frac{a}{h}, b_D = \frac{b}{h} \tag{6}$$

$$t_D = \frac{Kt}{\phi \mu C_t h^2} \tag{7}$$

$$P_D = \frac{2\pi Kh(P_{ini} - P)}{\mu B q_{ref}} \tag{8}$$

$$q_D(t_D) = \frac{2\pi q(t)}{q_{ref}} \tag{9}$$

where P_{ini} is initial reservoir pressure, q_{ref} is the reference flow rate.

Consequently, the dimensionless governing equation can be denoted as follows:

$$\frac{\partial P_D}{\partial t_D} - \left(\frac{\partial^2 P_D}{\partial x_D^2} + \frac{\partial^2 P_D}{\partial y_D^2}\right) = q_D(t_D)\delta(x_D - x_{wD})\delta(y_D - y_{wD}) \tag{10}$$

And then, the dimensionless boundary conditions, initial condition, dimensionless wellbore pressure can be expressed as follows:

$$\frac{\partial P_D}{\partial t_D}|_{x=0,a_D} = \frac{\partial P_D}{\partial y_D}|_{y=0,b_D} = \frac{\partial P_D}{\partial z_D}|_{z=0,h_D} = 0 \tag{11}$$

$$P_D(x_D, y_D)|_{t_D=0} = 0 \tag{12}$$

$$P_D(t_D, x_{wD}, y_{wD}) = P_{wD} \tag{13}$$

2.4 Laplace transform

In order to solve equations in real space, it is quite convenient to process the equation in the Laplace transform space. Considering the initial condition Eq. (12), taking the Laplace transform with respect to t_D at the both sides of Eq. (10), we obtain (Tuma, 1997; Lu at al, 2018):

$$s\hat{P}_D - \left(\frac{\partial^2 \hat{P}_D}{\partial x_D^2} + \frac{\partial^2 \hat{P}_D}{\partial y_D^2}\right) = \hat{q}_D(s)\delta(x_D - x_{wD})\delta(y_D - y_{wD}) \tag{14}$$

where s is the Laplace transform variable with respect to t_D.

Through the superposition principle (Lee et al, 2003; Lu et al, 2019), we can easily obtain the solution of Eq. (14) as below:

$$\hat{P}_D(s, x_D, y_D) = \hat{q}_D(s) G(s, x_D, y_D; x_{wD}, y_{wD}) \tag{15}$$

where (Stakgold, 1998; Cole et al, 2011)

$$G(s,x_D,y_D;x_{wD},y_{wD}) = \frac{\sum_{u=0}^{\infty}\sum_{v=0}^{\infty} \cos\left(\frac{u\pi x_D}{a_D}\right)\cos\left(\frac{v\pi y_D}{b_D}\right)\cos\left(\frac{u\pi x_{wD}}{a_D}\right)\cos\left(\frac{u\pi Y_{wD}}{B_D}\right)}{(a_D b_D d_u d_v)(s+\lambda_{uv})} \tag{16}$$

$$d_u = \begin{cases} 1, & \text{if } u = 0 \\ \frac{1}{2}, & \text{if } u > 0 \end{cases}, d_v = \begin{cases} 1, & \text{if } v = 0 \\ \frac{1}{2}, & \text{if } v > 0 \end{cases} \tag{17}$$

$$\lambda_{uv} = \left(\frac{u\pi}{a_D}\right)^2 + \left(\frac{v\pi}{b_D}\right)^2 \tag{18}$$

Note that the flowing bottomhole pressure is constant, then in Eq. (15) we let $(x_D, y_D) = (x_{wD}, y_{wD} + r_{wD})$, there holds:

$$\frac{P_{wD}}{s} = \hat{q}_D(s)G(s, x_{wD}, y_{wD} + r_{wD}; x_{wD}, y_{wD}) \tag{19}$$

where

$$G(s, x_{wD}, y_{wD} + r_{wD}; x_{wD}, y_{wD}) = \frac{1}{(a_D b_D d_u d_v)(s + \lambda_{uv})} \times \sum_{u=0}^{\infty}\sum_{v=0}^{\infty}\left[\cos\left(\frac{u\pi x_D}{a_D}\right)\cos\left(\frac{v\pi(y_{wD}+r_{wD})}{b_D}\right)\cos\left(\frac{u\pi x_{wD}}{a_D}\right)\cos\left(\frac{v\pi y_{wD}}{b_D}\right)\right] \tag{20}$$

Note that Eq. (16) can be simplified as below:

$$G(s, x_D, y_D; x_{wD}, y_{wD}) = \sum_{u=0}^{\infty}\left\{\cos\left(\frac{u\pi x_D}{a_D}\right)\cos\left(\frac{u\pi x_{wD}}{a_D}\right)\{\cosh[w_u(b_D - |y_D - y_{wD}|)] + \cosh[w_u(b_D - y_D - y_{wD})]\}\right\} \times \frac{1}{(2a_D d_u \omega_u)\sinh(\omega_u b_D)} \tag{21}$$

and

$$\omega_u = \left[s + \left(\frac{u\pi}{a_D}\right)^2\right]^{1/2} \tag{22}$$

Consequently,

$$G(s, x_{wD}, y_{wD} + r_{wD}; x_{wD}, y_{wD}) = \sum_{u=0}^{\infty}\left[\cos\left(\frac{u\pi x_{wD}}{a_D}\right)\right]^2 \times \{\cosh[w_u(b_D - r_{wD})] + \cosh[w_u(b_D - 2y_{wD})]\} \times \frac{1}{(2a_D d_u \omega_u)\sinh(\omega_u b_D)} \tag{23}$$

From Eq. (19), we obtain:

$$\hat{q}_D(s) = \frac{P_{wD}}{sG(s, x_{wD}, y_{wD} + r_{wD}; x_{wD}, y_{wD})} \tag{24}$$

2.5 Pressure distribution

According to Eqs. (19) and (24), the dimensionless pressure at point (x_D, y_D) at time t_D can be expressed below:

$$P_D(x_D, y_D, t_D) = \int_0^{t_D} G(t_D, x_D, y_D; \tau x_{wD}, y_{wD}) q_D(\tau) d\tau \tag{25}$$

where (Stakgold, 1998; Cole et al, 2011)

$$\begin{aligned} G(t_D, x_D, y_D, \tau, x_{wD}, y_{wD}) = \frac{1}{a_D b_D} \times \{1 &+ 2\sum_{m=1}^{\infty}\exp\left[\frac{-m^2\pi^2(t_D-\tau)}{a_D^2}\right]\cos\left(\frac{m\pi x_D}{a_D}\right)\cos\left(\frac{m\pi x_{wD}}{a_D}\right) \\ &+ 2\sum_{n=1}^{\infty}\exp\left[\frac{-n^2\pi^2(t_D-\tau)}{b_D^2}\right]\cos\left(\frac{n\pi y_D}{b_D}\right)\cos\left(\frac{n\pi y_{wD}}{b_D}\right) \\ &+ 4\sum_{m=1}^{\infty}\sum_{n=1}^{\infty}\exp\left[\left(\frac{-m^2\pi^2}{a_D^2} - \frac{n^2\pi^2}{b_D^2}\right)(t_D - \tau)\right]\cos\left(\frac{m\pi x_D}{a_D}\right) \\ &\cos\left(\frac{m\pi x_{wD}}{a_D}\right)\cos\left(\frac{n\pi y_D}{b_D}\right)\cos\left(\frac{n\pi y_{wD}}{b_D}\right)\} \end{aligned} \tag{26}$$

If the well is produced at a constant flow rate q, Eq. (25) can be simplified, then the dimensionless pressure distribution in the rectangular-shaped reservoir is expressed below:

$$\begin{aligned} P_D(t_D, x_D, y_D) = \frac{q_D}{a_D b_D} &\times \left\{t_D + 2\sum_{m=1}^{\infty}\left(\frac{a_D^2}{m^2\pi^2}\right)\left[1 - \exp\left(\frac{-m^2\pi^2 t_D}{a_D^2}\right)\right]\right. \\ &\cos\left(\frac{m\pi x_D}{a_D}\right)\cos\left(\frac{m\pi x_{wD}}{a_D}\right) \\ &+ 2\sum_{n=1}^{\infty}\left(\frac{b_D^2}{n^2\pi^2}\right)\left[1 - \exp\left(\frac{-n^2\pi^2 t_D}{b_D^2}\right)\right]\cos\left(\frac{n\pi y_D}{b_D}\right) \\ &\cos\left(\frac{m\pi y_{wD}}{b_D}\right) \\ &+ 4\sum_{m=1}^{\infty}\sum_{n=1}^{\infty}\left(\frac{1}{m^2\pi^2/a_D^2 + n^2\pi^2/b_D^2}\right) \\ &\left\{1 - \exp\left[\left(\frac{-m^2\pi^2}{a_D^2} - \frac{n^2\pi^2}{b_D^2}\right)t_D\right]\right\}\cos\left(\frac{m\pi x_D}{a_D}\right) \\ &\left.\cos\left(\frac{m\pi x_{wD}}{a_D}\right)\cos\left(\frac{n\pi y_D}{b_D}\right)\cos\left(\frac{n\pi y_{wD}}{b_D}\right)\right\} \end{aligned} \tag{27}$$

where

$$q_D = \frac{2\pi q}{q_{ref}} \tag{28}$$

2.6 Pressure buildup after the well is shut-in

Recall Eq. (25), if the well is produced at a constant flowing bottomhole pressure P_w, then at the wellbore, there holds:

$$P_{wD} = \int_0^{t_D} G(t_D, x_{wD}, y_{wD}, \tau) q_D(\tau) d\tau \tag{29}$$

where (Zwillinger, 1996; Stakgold, 1998)

$$\begin{aligned} G(t_D, x_{wD}, y_{wD}, \tau) = \frac{1}{a_D b_D} &\times \left\{1 + 2\sum_{m=1}^{\infty}\exp\left[\frac{-m^2\pi^2(t_D-\tau)}{a_D^2}\right]\cos^2\left(\frac{m\pi x_{wD}}{a_D}\right)\right. \\ &+ 2\sum_{n=1}^{\infty}\exp\left[\frac{-n^2\pi^2(t_D-\tau)}{b_D^2}\right]\cos^2\left(\frac{n\pi y_{wD}}{b_D}\right) \\ &+ 4\sum_{m=1}^{\infty}\sum_{n=1}^{\infty}\exp\left[\left(\frac{-m^2\pi^2}{a_D^2} - \frac{n^2\pi^2}{b_D^2}\right)(t_D - \tau)\right] \\ &\left.\cos^2\left(\frac{m\pi x_{wD}}{a_D}\right)\cos^2\left(\frac{n\pi y_{wD}}{b_D}\right)\right\} \end{aligned} \tag{30}$$

Take the Laplace transform with respect to t_D at both sides of Eq. (30), we obtain:

$$\begin{aligned} P_{wD}/s = \frac{\hat{q}_D(s)}{a_D b_D}&\left\{1 + 2\sum_{m=1}^{\infty}\left(\frac{1}{s + m^2\pi^2/a_D^2}\right)\cos^2\left(\frac{m\pi x_{wD}}{a_D}\right)\right. \\ &+ 2\sum_{n=1}^{\infty}\left(\frac{1}{s + n^2\pi^2/b_D^2}\right)\cos^2\left(\frac{n\pi y_{wD}}{b_D}\right) \\ &+ 4\sum_{m=1}^{\infty}\sum_{n=1}^{\infty}\exp\left[\left(\frac{1}{s + m^2\pi^2/a_D^2 + n^2\pi^2/b_D^2}\right.\right. \\ &\left.(t_D - \tau)\right]\cos^2\left(\frac{m\pi x_{wD}}{a_D}\right)\cos^2\left(\frac{n\pi y_{wD}}{b_D}\right)\right\} \end{aligned} \tag{31}$$

Consequently,

$$\hat{q}_D(s) = \frac{a_D b_D P_{wD}}{s f(s)} \tag{32}$$

where

$$f(s) = 1 + 2\sum_{m=1}^{\infty}\left(\frac{1}{s+m^2\pi^2/a_D^2}\right)\cos^2\left(\frac{m\pi x_{wD}}{a_D}\right) + 2\sum_{n=1}^{\infty}\left(\frac{1}{s+n^2\pi^2/b_D^2}\right)\cos^2\left(\frac{n\pi y_{wD}}{b_D}\right) + 4\sum_{m=1}^{\infty}\sum_{n=1}^{\infty}\left(\frac{1}{s+m^2\pi^2/a_D^2+n^2\pi^2/b_D^2}\right)\cos^2\left(\frac{m\pi x_{wD}}{a_D}\right)\cos^2\left(\frac{n\pi y_{wD}}{b_D}\right) \tag{33}$$

If the well is produced at a constant flowing bottomhole pressure P_w, and the well is shut-in at time $t = t_p$, when $t > t_p$, then at the total dimensionless time t_D, the dimensionless shut-in time is $\Delta t_D = t_D - t_{pD}$, and the dimensionless shut-in bottomhole pressure is given below:

$$P_{wsD}(t_D, t_{pD}) = \int_0^{t_{pD}} G(t_D, x_{wD}, y_{wD}, \tau) q_D(\tau) d\tau \tag{34}$$

Applying Gaussian quadrature (Zwillinger, 1996), taking the change of variables as below:

$$\tau = \frac{t_{pD} + t_{pD}\xi}{2} = \frac{t_{pD}}{2}(1+\xi) \tag{35}$$

$$d\tau = \frac{t_{pD}}{2} d\xi \tag{36}$$

then Eq. (34) can be expressed as:

$$\begin{aligned} P_{wD}(t_D, t_{pD}) &= \int_0^{t_{pD}} q_D(\tau) G(t_D, x_{wD}, y_{wD}, \tau) d\tau \\ &= \int_{-1}^{1} q_D\left[\frac{t_{pD}}{2}(1+\xi)\frac{1}{a_D b_D}\right] \\ &\left\{2\sum_{m=1}^{\infty}\exp\left\{-m^2\pi^2\left[t_D - \frac{t_{pD}}{2}(1+\xi)\right]/a_D^2\right\}\cos^2\frac{m\pi x_{wD}}{a_D}\right. \\ &+2\sum_{n=1}^{\infty}\exp\left(-n^2\pi^2\left(t_D - \frac{t_{pD}}{2}(1+\xi)\right)/b_D^2\right)\cos^2\frac{n\pi y_{wD}}{b_D}\Bigg] \\ &+4\sum_{m=1}^{\infty}\sum_{n=1}^{\infty}\exp\left\{\left(\frac{-m^2\pi^2}{a_D^2} - \frac{n^2\pi^2}{b_D^2}\right)\left[t - \frac{t_{pD}}{2}(1+\xi)\right]\right\} \\ &\left.\cos^2\left(\frac{m\pi x_{wD}}{a_D}\right)\cos^2\left(\frac{n\pi y_{wD}}{b_D}\right)\right\}\frac{t_{pD}}{2}d\xi \end{aligned} \tag{37}$$

Applying Gaussian quadrature with 100 points (Zwillinger, 1996) to approximate the integral in Eq. (37), the dimensionless shut-in bottomhole pressure is given by:

$$P_{wsD}(t_D, t_{pD}) = \frac{t_{pD}}{2a_D b_D}\sum_{k=1}^{100}\lambda_k q_D\left[\frac{t_{pD}}{2}(1+\xi_k)\right] f(t_{pD}, \xi_k) \tag{38}$$

where

$$\begin{aligned} f(t_{pD}, \xi_k) \approx &\left\{1 + 2\sum_{m=1}^{200}\exp\left\{-m^2\pi^2\left[t_D - \frac{t_{pD}}{2}(1+\xi_k)\right]/a_D^2\right\}\right. \\ &\times\cos^2\frac{m\pi x_{wD}}{a_D} \\ &+2\sum_{n=1}^{200}\exp\left\{-n^2\pi^2\left[t_D - \frac{t_{pD}}{2}(1+\xi_k)\right]/b_D^2\right\}\cos^2\frac{n\pi y_{wD}}{b_D} \\ &+4\sum_{m=1}^{\infty}\sum_{n=1}^{\infty}\exp\left\{\left(\frac{-m^2\pi^2}{a_D^2} - \frac{n^2\pi^2}{b_D^2}\right)\left[t - \frac{t_{pD}}{2}(1+\xi_k)\right]\right\} \\ &\left.\cos^2\left(\frac{m\pi x_{wD}}{a_D}\right)\cos^2\left(\frac{n\pi y_{wD}}{b_D}\right)\right\} \end{aligned} \tag{39}$$

Note that ξ_k and λ_k are the nodes and the corresponding weighting factors of Gaussian quadrature (Zwillinger, 1996).

Eq. (38) gives the algorithm to calculate the shut-in bottomhole pressure if a well producing at constant bottomhole pressure prior to shut-in in a closed rectangular-shaped reservoir.

If the well is produced at a constant flow rate q, and the well is shut-in at time $t = t_p$, when $t > t_p$, then at the total dimensionless time t_D, dimensionless shut-in time is $\Delta t_D = t_D - t_{pD}$, the dimensionless shut-in bottomhole pressure is given by:

$$P_{wsD}(t_D, t_{pD}) = q_D\int_0^{t_{pD}} G(t_D, x_{wD}, y_{wD}, \tau) d\tau \tag{40}$$

Eq. (40) is equivalent to the equation below:

$$P_{wsD}(t_D, t_{pD}) = q_D\int_{t_D - t_{pD}}^{t_D} G(\tau, x_{wD}, y_{wD}) d\tau \tag{41}$$

where (Stakgold, 1998; Cole et al, 2011)

$$\begin{aligned} G(\tau, x_{wD}, y_{wD}) = &\frac{1}{a_D b_D} \\ &\times\left\{1 + 2\sum_{m=1}^{\infty}\exp\left(-m^2\pi^2\tau/a_D^2\right)\cos^2\left(\frac{m\pi x_{wD}}{a_D}\right)\right. \\ &+2\sum_{n=1}^{\infty}\exp\left(-n^2\pi^2\tau/b_D^2\right)\cos^2\left(\frac{n\pi y_{wD}}{b_D}\right) \\ &+4\sum_{m=1}^{\infty}\sum_{n=1}^{\infty}\exp\left[\left(\frac{-m^2\pi^2}{a_D^2} - \frac{n^2\pi^2}{b_D^2}\right)\tau\right]\cos^2\left(\frac{m\pi x_{wD}}{a_D}\right) \\ &\left.\cos^2\left(\frac{n\pi y_{wD}}{b_D}\right)\right\} \end{aligned} \tag{42}$$

So, the dimensionless shut-in bottom hole pressure is:

$$\begin{aligned} P_{wsD}(t_D, t_{pD}) \approx &\frac{q_D t_{pD}}{a_D b_D} + \frac{2q_D}{a_D b_D}\sum_{m=1}^{200}\cos^2\left(\frac{m\pi x_{wD}}{a_D}\right)\frac{a_D^2}{m^2\pi^2} \\ &\times\left\{-\exp\left(\frac{-m^2\pi^2 t_D}{a_D^2}\right) + \exp\left[\frac{-m^2\pi^2(t_D - t_{pD})}{a_D^2}\right]\right\} \\ &+\frac{2q_D}{a_D b_D}\sum_{m=1}^{200}\cos^2\left(\frac{m\pi y_{wD}}{b_D}\right)\frac{b_D^2}{n^2\pi^2}\left\{-\exp\left(\frac{-n^2\pi^2 t_D}{b_D^2}\right)\right. \\ &\left.+\exp\left[\frac{-n^2\pi^2(t_D - t_{pD})}{b_D^2}\right]\right\} \\ &+\frac{4q_D}{a_D b_D}\sum_{m=1}^{200}\sum_{n=1}^{200}\left(\frac{1}{m^2\pi^2/a_D^2 + n^2\pi^2/b_D^2}\right)\cos^2\left(\frac{m\pi x_{wD}}{a_D}\right) \\ &\cos^2\left(\frac{n\pi y_{wD}}{b_D}\right)\left\{\exp\left[\left(\frac{-m^2\pi^2}{a_D^2} - \frac{n^2\pi^2}{b_D^2}\right)(t_D - t_{pD})\right] - \right. \\ &\left.\exp\left[\left(\frac{-m^2\pi^2}{a_D^2} - \frac{n^2\pi^2}{b_D^2}\right)t_D\right]\right\} \end{aligned} \tag{43}$$

Table 1. Reservoir and fluid properties data.

Reservoir domain, Ω	500 m $\times$ 500 m
Initial reservoir pressure, P_{ini}	25 MPa
Flowing bottomhole pressure, P_{wf}	20 MPa
Formation volume factor, B	1.15 Rm^3/Sm^3
Reservoir thickness, h	25 m
Reservoir porosity, ϕ	0.15
Reservoir permeability, K	0.1 μm^2
Total reservoir compressibility, C_t	3.0×10^{-3} MPa^{-1}
Oil viscosity, μ	5 mPa·s
Production time prior to shut-in, t_p	720 hours
Wellbore radius, r_w	0.1 m

Eq. (43) gives the algorithm to calculate the shut-in bottomhole pressure if a well producing at constant flow rate prior to shut-in in a closed rectangular-shaped reservoir.

3. Validation

Computer Modeling Group Ltd., abbreviated as CMG, develops market-leading reservoir simulation software, which is known as the industry standard for advanced recovery processes. In this paper, the CMG Black oil simulator IMEX is used to build and run the simulation. And we will use the proposed analytical model to investigate the pressure buildup of a well in a closed square-shaped reservoir, as shown in Fig. 1. The input reservoir data, formation properties data, fluid properties data and production time prior to shut-in are shown in Table 1. The lower left point of the square is the origin point of the Cartesian coordinate system, as shown in Fig. 1. Assume the well is at (250 m, 250 m), i.e. the well is located at the center of the square-shaped reservoir.

Assume the well has produced for 720 hours at the constant bottomhole pressure of 20 MPa prior to shut-in, and the production pressure difference (initial reservoir pressure minus flowing bottomhole pressure) keeps a constant during production, $P_{ini} - P_{wf} = \Delta P_w = 5$ MPa.

By using the IMEX simulator, we can obtain the shut-in bottomhole pressure. Through the proposed model, we can calculate the dimensionless shut-in bottomhoe pressure in the same case as the CMG simulation. Recall Eqs. (7) and (8), if we use practical units, (h in m; μ in mPa·s; K in μm^2; C_t in MPa^{-1}; t in hours; q_{ref} in Sm^3/day, P in MPa) then the dimensionless shut-in time Δt_D and the dimensionless shut-in bottomhole pressure P_{wsD} can be converted to the shut-in time and the shut-in bottomhole pressure as below:

$$\Delta t = \frac{\phi \mu C_t h^2 \Delta t_D}{3.6K}, \tag{44}$$

$$P_{ws} = P_{ini} - \frac{1.842 \times 10^{-3} \mu B q_{ref} P_{wsD}}{Kh} \tag{45}$$

Then, the calculated shut-in bottomhole pressure and the shut-in bottomhole pressure obtained by the CMG simulation can be compared, as shown in Fig. 2.

$$P_{wsD}(t_D, t_{pD}) = q_D \int_{t_D - t_{pD}}^{t_D} G(\tau, x_{wD}, y_{wD}) d\tau \tag{46}$$

It can be found from Fig. 2 that the shut-in bottomhole pressure predicted by the proposed model is basically consistent with the overall trend of the shut-in bottomhole pressure obtained by the CMG simulation over time, indicating that the results predicted by the proposed model are reliable within a certain range. Since we ignore high order term in the model development, and the numerical inverse Laplace transform method proposed by Stehfest (1970) is an approximate method, consequently, there exist some differences between the CMG simulation and the proposed model results, but the differences are not significant.

4. Application and analysis

In this part, we will use the proposed model to study the effects of reservoir boundary condition, reservoir size, well location, production pressure difference and production time prior to shut-in on the shut-in bottomhole pressure.

4.1 The effect of reservoir boundary condition

Example 1: We study the effect of reservoir boundary condition on shut-in bottomhole pressure. The formation properties data, fluid properties data and production time prior to shut-in are the same as those given in Table 1, and the production pressure difference keeps a constant during production, $\Delta P_w = 5$ MPa. Calculate the shut-in bottomhole pressure in the following cases: (1) A well in an infinite reservoir; (2) A well at the center of a closed square-shaped reservoir with side length 500 m.

For Case 1, the algorithm to calculate the shut-in bottomhole pressure for a well producing at constant bottomhole pressure prior to shut-in in an infinite reservoir is given by Lu at al (2018). For Case 2, Eq. (38) is used to calculate the shut-in bottomhole pressure of the well producing at constant bottomhole pressure prior to shut-in in the closed square-shaped reservoir.

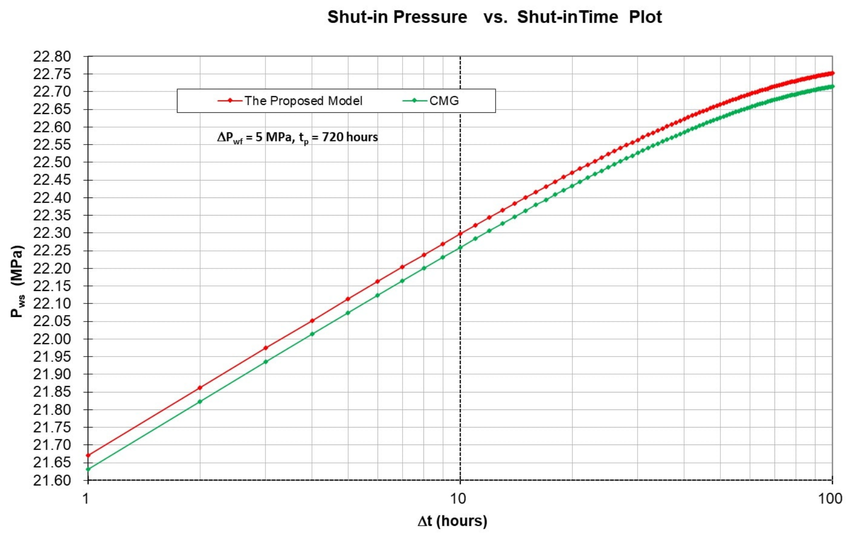

Fig. 2. Comparison of the shut-in pressure obtained by the CMG simulation and the proposed model of Well A.

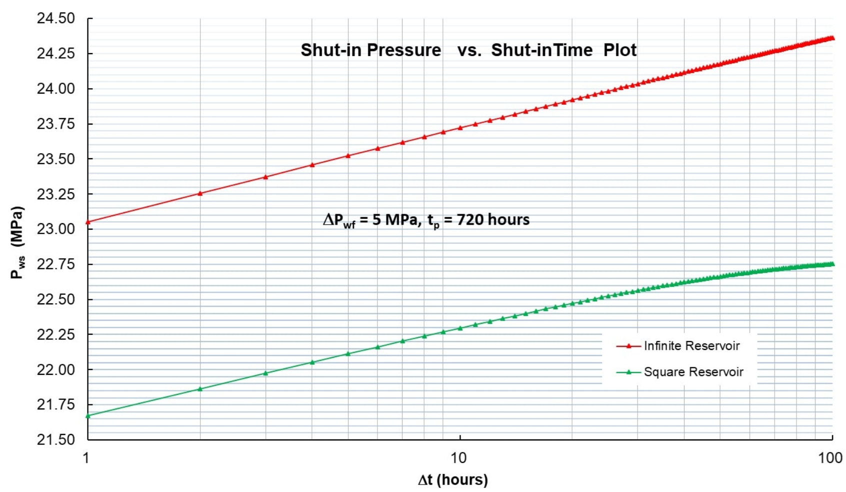

Fig. 3. Effect of reservoir boundary condition on shut-in bottomhole pressure.

The shut-in bottomhole of the well in the above two cases are shown in Fig. 3.

As can be seen from Fig. 3, at a given shut-in time, the shut-in bottomhole pressure for an infinite reservoir is larger than that for a closed square-shaped reservoir. An infinite reservoir has a larger drainage area than a closed square reservoir, consumes less energy for the same production pressure difference before shut-in and the same production time, and therefore the infinite reservoir recovers pressure faster after shut-in. Consequently, at the same shut-in time, the shut-in bottomhole pressure of the infinite reservoir is greater than that of the closed square reservoir, and the differences are significant.

4.2 The effect of reservoir size

Example 2: We study the effect of reservoir size on shut-in bottomhole pressure. The formation properties data, fluid properties data and production time prior to shut-in are the same as those given in Table 1, and the production pressure difference keeps a constant during production, ΔP_w = 5 MPa. A well is located at the center of a closed square-shaped reservoir. Calculate the shut-in bottomhole pressure in the following cases: (1) Reservoir side length is 400 m; (2) Reservoir side length is 500 m; (3) Reservoir side length is 600 m.

The shut-in bottomhole of the well in the above three cases are shown in Fig. 4.

As can be seen from Fig. 4, at a given shut-in time, the larger the reservoir size, the larger value of shut-in

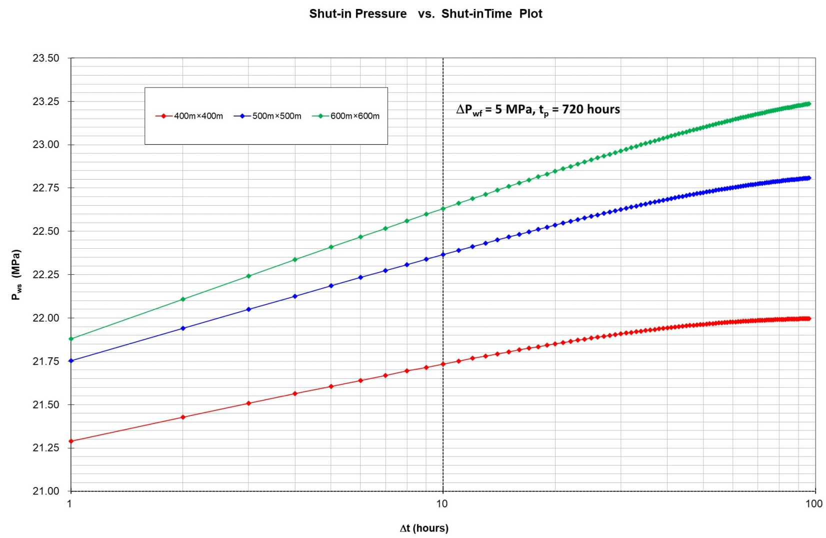

Fig. 4. Effect of reservoir size on shut-in bottomhole pressure.

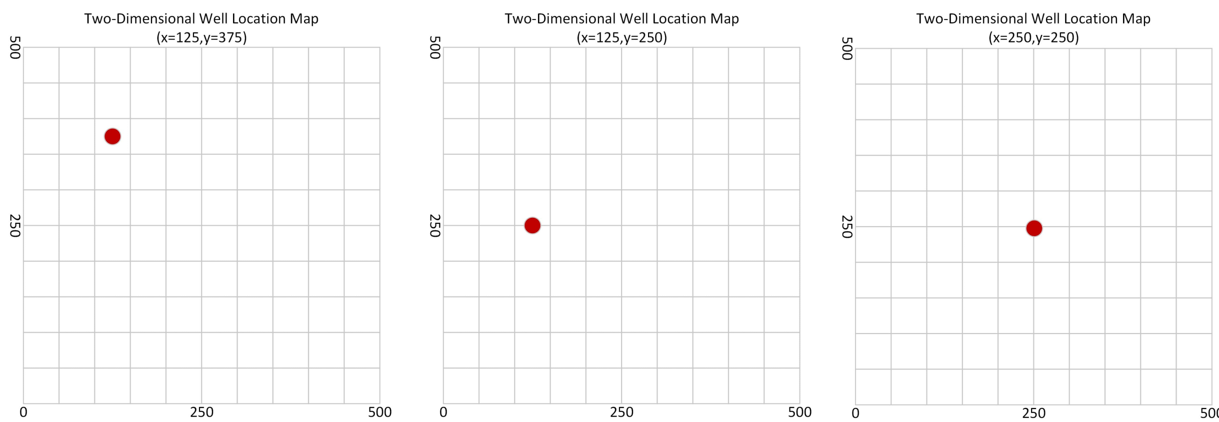

Fig. 5. Well location map.

bottomhole pressure. Fig. 4 shows that the reservoir size has significant influence on pressure buildup behavior. Large reservoir size means large drainage area. A well in a larger drainage area consumes less energy for the same production pressure difference before shut-in and the same production time, consequently, at the same shut-in time, the shut-in bottomhole pressure of the larger reservoir is greater than that of the smaller reservoir.

4.3 The effect of well location

Example 3: We study the effect of well location on shut-in bottomhole pressure. The production pressure difference keeps a constant during production, ΔP_w = 5 MPa. The reservoir data, formation properties and fluid properties data are the same as those given Table 1. The lower left point of the square is the origin point of the Cartesian coordinate system, as shown in Fig. 1. Calculate the shut-in bottomhole pressure in the following cases: (1) the well at (125 m, 375 m); (2) the well at (125 m, 250 m); (3) the well at (250 m, 250 m).

The well locations are shown in Fig. 5. The shut-in bottomhole of the well in the above three cases are shown in Fig. 6. As can be seen from Fig. 6, at a given shut-in time, the shut-in bottomhole pressure for the well located at the center of the closed square-shaped reservoir (Case 3) is the largest, the shut-in bottomhole pressure for the well at (125 m, 375 m) (Case 1) is the smallest.

Because in a closed square-shaped reservoir, no driving force is from outer boundary, for the well located at the center (Case 3) , all flowlines towards to the wellbore are radial during production, no curved flowlines, the well consumes least energy for the same production pressure difference before shut-in and the same production time, the speed of reservoir pressure recovery is the fastest after shut-in, consequently, at the same shut-in time, the shut-in bottomhole pressure is the largest in Case 3. The well is not located at the center in Case 1 and Case 2, the flowlines towards to the wellbore are curved during production, more energy is dissipated under the same production pressure difference, the speed of reservoir pressure recovery in Case 1 and Case 2 is smaller than that in Case 3,

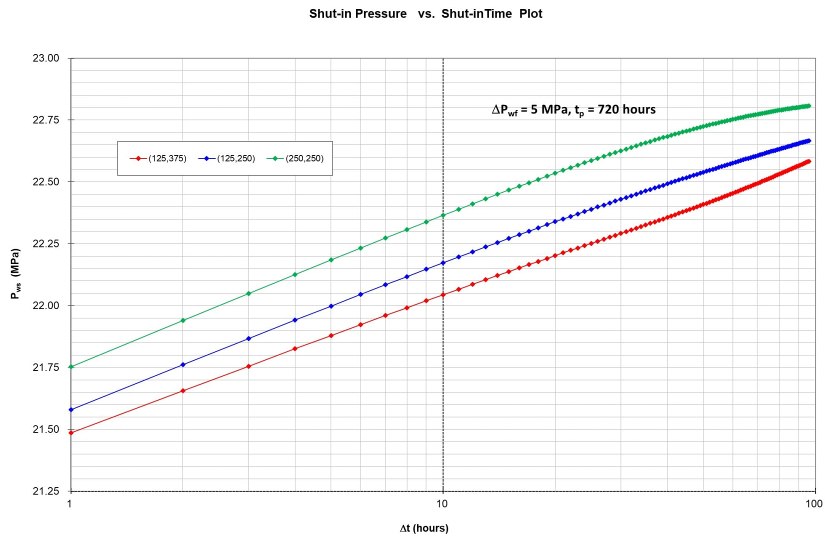

Fig. 6. Effects of well location on shut-in bottomhole pressure.

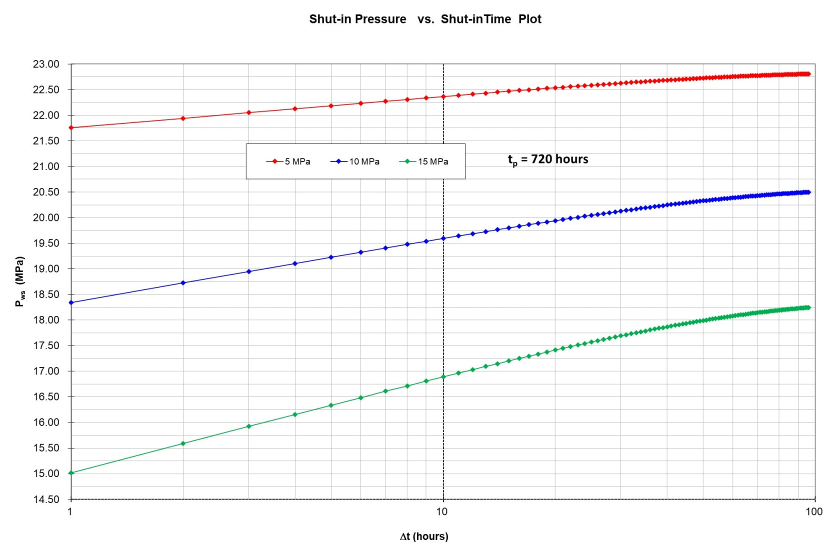

Fig. 7. Effect of production pressure difference on shut-in bottomhole pressure.

consequently, at the same shut-in time, the shut-in bottomhole pressure is smaller. In Case 1, the distance between the well and upper boundary is smaller than the distance between the well and lower boundary, which leads to the increase of curvature of flowlines and increase of reservoir energy consumption during production, consequently, the speed of reservoir pressure recovery is the smallest after shut-in, at the same shut-in time, the shut-in bottomhole pressure is the smallest in Case 1.

Fig. 6 shows that the well location has significant effect on pressure buildup behavior.

4.4 The effect of production pressure difference

Example 4: We study the effect of production pressure difference on shut-in bottomhole pressure. The reservoir data, formation properties data, fluid properties data and production time prior to shut-in are the same as those given in Table 1. The well is at the center of the reservoir, i.e. the well at (250 m, 250 m). Calculate the shut-in bottomhole pressure in the following cases: (1) Production pressure difference $P_{ini} - P_{wf} = \Delta P_w = 5$ MPa; (2) $P_{ini} - P_{wf} = \Delta P_w = 10$ MPa; (3) $P_{ini} - P_{wf} = \Delta P_w = 15$ MPa.

The shut-in bottomhole of the well in the above three cases are shown in Fig. 7. As can be seen from Fig. 7, at a given shut-in time, with the increase of production pressure difference prior to shut-in, the energy consumption degree of the reservoir increases during production, consequently, the speed of reservoir pressure recovery decreases after shut-in.

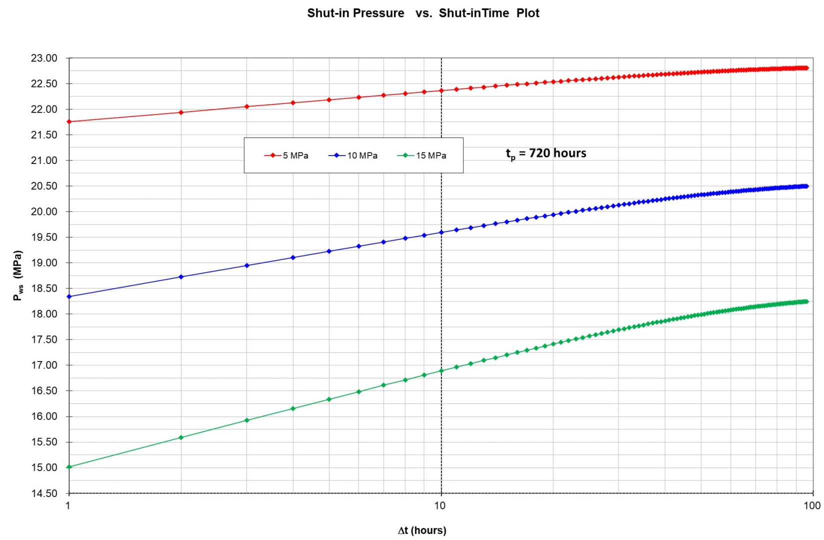

Fig. 8. Effect of production time on shut-in bottomhole pressure.

Thus, at the same shut-in time, the smaller production pressure difference prior to shut-in, the larger the shut-in bottomhole pressure. The shut-in bottomhole pressure in Case 1 (ΔP_w = 5 MPa) is the largest, the shut-in bottomhole pressure in Case 3 (ΔP_w = 15 MPa) is the smallest.

Fig. 7 shows that the production pressure difference prior to shut-in has significant effect on pressure buildup behavior.

4.5 The effect of well production time prior to shut-in

Example 4: We study the effect of well production time prior to shut-in on shut-in bottomhole pressure. The production pressure difference keeps a constant during production, ΔP_w=5 MPa. The reservoir data, formation properties and fluid properties data are the same as those given Table 1. Calculate the shut-in bottomhole pressure in the following cases: (1) production time prior to shut-in t_p = 720 hours; (2) t_p = 960 hours; (3) t_p = 1200 hours.

The shut-in bottomhole of the well in the above three cases are shown in Fig. 8. As can be seen from Fig. 8, with the increase of production time prior to shut-in, the energy consumption degree of the reservoir increases during production, consequently, the speed of reservoir pressure recovery decreases after shut-in. Thus, at the same shut-in time, the smaller production time prior to shut-in, the larger the shut-in bottomhole pressure. The shut-in bottomhole pressure in Case 1 (t_p = 720) is the largest, the shut-in bottomhole pressure in Case 3 (t_p = 1200) is the smallest.

Fig. 8 shows that the production time prior to shut-in has significant effect on pressure buildup behavior.

5. Conclusions

Compared with the empirical or semi-analytical models in the literature, our proposed model in this paper has a solid theoretical basis, the proposed analytical model provides a computationally efficient, accurate and convenient method for predicting pressure buildup behavior of a well produced at constant bottomhole pressure prior to shut-in in a closed rectangular-shaped reservoir. Comparing with the results in the CMG simulation, it is found that the proposed model is accurate enough to predict the pressure buildup behavior. Also, the reservoir boundary condition, the reservoir size, the well location, the production pressure difference and the well production time prior to shut-in have significant effects on the pressure buildup behavior.

The following conclusions can be reached:

- A well in a larger drainage area consumes less energy for the same production pressure difference before shut-in and the same production time, at the same shut-in time, the shut-in bottomhole pressure of the larger reservoir is greater than that of the smaller reservoir.
- Compared with an off-center well, a well located at the center of the drainage area consumes less energy for the same production pressure difference before shut-in and the same production time, the speed of reservoir pressure recovery is faster after shut-in, at the same shut-in time, the shut-in bottomhole pressure is larger.
- If the production time is the same, with the increase of production pressure difference prior to shut-in, the energy consumption degree of the reservoir increases during production, consequently, the speed of reservoir pressure recovery decreases after shut-in, at the same shut-in time, the smaller production pressure difference prior to shut-in, the larger the shut-in bottomhole pressure.
- If the production pressure difference is the same, with the increase of production time prior to shut-in, the energy consumption degree of the reservoir increases during production, consequently, the speed of reservoir pressure recovery decreases after shut-in, at the same shut-in time, the smaller production time prior to shut-in, the larger the

shut-in bottomhole pressure.

Nomenclature

a = Length of rectangular reservoir, m
a_D=Dimensionless length of rectangular reservoir
b = Width of rectangular reservoir, m
b_D=Dimensionless width of rectangular reservoir
B = Formation volume factor, Rm^3/Sm^3
C_t = Total reservoir compressibility, MPa^{-1}
h =Formation thickness, m
K =Reservoir permeability, μm^2
P =Pressure, MPa
P_{ini} =Initial reservoir pressure, MPa
P_w =Flowing bottombore pressure, MPa
P_{ws} =Shut-in bottomhole pressure, MPa
P_D =Dimensionless pressure
P_{wD} =Dimensionless flowing bottombore pressure
P_{wsD} =Dimensionless shut-in bottombore pressure
$\hat{P}_D$ =Dimensionless pressure in Laplace transform space
q =Flow rate, Sm^3/day
q_D =Dimensionless flow rate
$\hat{q}_D$ =Dimensionless flow rate in Laplace transform space
q_{ref} =Reference flow rate, Sm^3/day
r =Radial distance, m
r_D =Dimensionless radial distance
r_w =Wellbore radius, m
r_{wD} =Dimensionless wellbore radius
t =Time, hour
t_p =Production time prior to shut-in, hour
Δt =Well shut-in time, hour
t_D =Dimensionless time
t_{pD} =Dimensionless production time prior to shut-in
Δt_D =Dimensionless well shut-in time
x_w =Coordinate in X direction of well in rectangular reservoir, m
x_{wD} =Dimensionless coordinate in X direction of well in rectangular reservoir
y_w =Coordinate in Y direction of well in rectangular reservoir, m
y_{wD} =Dimensionless coordinate in Y direction of well in rectangular reservoir

Greek symbols

μ =Fluid viscosity, mPa·s
ϕ =Porosity
λ_{uv} =A function defined by Eq. (18)
ω_u =A function defined by Eq. (22)

Subscripts

D = Dimensionless
ini =Initial
ws =Shut-in bottomhole

Acknowledgements

Authors acknowledge the financial support from the “Local Universities Reformation and Development Personnel Training Project from Central Authorities Study on nanosystem displacement method of tight reservoir in Daqing Oilfield”, and National Natural Science Foundation of China (NSFC) under grant No.52274037, and the Hainan Province Science and Technology Special Fund under grant No. ZDYF2022SHFZ107.

Conflict of interest

The authors declare no competing interest.

References

Bossie-Codreanu, D. A simple buildup analysis method to determine well drainage area and drawdown pressure for a stabilized well. Paper SPE 15977 Presented at Formation Evaluation, September, 1989.

Camacho-V, R., Galindo-N, A., Prats, M. Buildup solution in a system with multiple wells producing at constant wellbore pressures. Paper SPE 79104 Presented at Reservoir Evaluation and Engineering, August, 2002.

Chen, H. K., Brigham, W. E. Pressure buildup for a well with storage and skin in a closed square. Journal of Petroleum Technology, 1978, 30(1): 141-146.

Clegg, M. W. Some approximate solutions of radial flow problems associated with production at constant well pressure. Paper SPE 1536 Presented at Society of Petroleum Engineers Journal, March, 1967.

Cobb, W. M., Smith, J. T. An Investigation of pressure-buildup tests in bounded Reservoirs. Paper SPE 5133 Presented at the Fall Meeting of the Society of Petroleum Engineers of AIME, Houston, Texas, 6–9 October, 1974.

Cole, K. D., Beck, J. V., Haji-Sheikh, A. Heat conduction using green’s functions. New York City, USA, CRC Press Taylor and Francis Group, 2011.

Deng, Q., Nie, R., Jia, Y., et al. A new method of pressure buildup analysis for a well in a multiwell reservoir. Paper SPE 175866 Presented at the SPE North Africa Technical Conference and Exhibition, Cairo, Egypt, 14–16 September, 2015.

Dietz, D. N. Determination of average reservoir pressure from build-up surveys. Paper SPE 1156 Presented at Journal of Petroleum Technology, August, 1965.

Ehlig-Economides, C. A., Ramey, H. J. Jr. Pressure buildup for wells produced at a constant pressure. Paper SPE 7985 Presented at Society of Petroleum Engineers Journal, February, 1981.

Guppy, K. H., Cinco-Ley, H., Ramey Jr, H. J. Pressure buildup analysis of fractured wells producing at high flow rates. Paper SPE 10178 Presented at Journal of Petroleum Technology, November, 1982.

Horner, D. R. Pressure buildup in wells. Paper WPC 4135 Presented at the 3rd World Petroleum Congress, The Hague, the Netherlands, May 28–June 6, 1951.

Hurst, W. Establishment of the skin effect and its impediment to fluid flow into a well bore. Petroleum Engineer, 1953, 25(11): B6-B16.

Kazemi, H. Determining average reservoir pressure from pressure buildup tests. Paper SPE 4052 Presented at Society of Petroleum Engineers Journal, 1974.

Kutasov, I. M. Application of the Horner method for a well produced at a constant bottomhole pressure. Paper SPE 15143 Presented at SPE Formation Evaluation, 1989.

Lee, J., Rollins, J. B., Spivey, J. P. Pressure transient testing. Society of Petroleum Engineers, Richardson, Texas, USA, 2003.

Lin, J., Yang, H. Pressure buildup analysis for a well in a closed, bounded multiwell reservoir. Chinese Journal of Chemical Engineering, 2005, 13(4): 441-450.

Lu, J., Owayed, J. F., Xu, J., et al. An analytical model on production performance of multiple wells producing at constant bottomhole pressures. Special Topics and Reviews in Porous Media-An International Journal, 2019, 10(1): 31-48.

Lu, J., Shi, S., Rahman, M. M. New mathematical models for production performance of a well producing at constant bottomhole pressure. Special Topics and Reviews in Porous Media-An International Journal, 2018, 9(3): 261-278.

Marhaendrajana, T., Blasingame, T. A. Decline curve analysis using type curves-evaluation of well performance behavior in a multiwell reservoir system. Paper SPE 71517 Presented at the SPE Annual Technical Conference and Exhibition, New Orleans, Louisiana, September 30–October 3, 2001.

Matthews, C. S., Brons, F., Hazebroek, P. A method for determination of average pressure in a bounded reservoir. Paper SPE 296 Presented at Transactions of the AIME, December, 1954.

Matthews, C. S. Analysis of pressure buildup and flow test data. Paper SPE 1631 Presented at Journal of Petroleum Technology, September, 1961.

Miller, C. C., Dyes, A. B., Hutchinson Jr, C. A. The estimation of permeability and reservoir pressure from bottom hole pressure build-up characteristics. Paper SPE 950091 Presented at Journal of Petroleum Technology, December, 1950.

Muskat, M. Use of data oil the build-up of bottom-hole pressures. Paper SPE 937044 Presented at Transactions of the AIME, December, 1937.

Ohaeri, C. U. Pressure buildup analysis for a well produced at a constant pressure in a naturally fractured reservoir. Paper SPE 12009 Presented at the SPE Annual Technical Conference and Exhibition, San Francisco, California, 5–8 October, 1983.

Olarewaju, J., Lee, W. J. Pressure buildup behavior of partially completed wells in layered reservoirs. Paper SPE 18876 Presented at the SPE Production Operations Symposium, Oklahoma City, Oklahoma, 13–14 March, 1989.

Onur, M., Serra, K.V., Reynolds, A. C. Analysis of pressure buildup data from a well in mutiwell system. Paper SPE 18123 Presented at SPE Formation Evaluation, March, 1991.

Prats, M., Meneses-P, L. L., Samaneigo-V, F., et al. Pressure buildup in a well produced at constant pressure. Paper SPE 201111 Presented at SPE Journal, December, 2020.

Ramey, H. J. Jr., Cobb, W. M. A general pressure buildup theory for a well in a closed drainage area. Paper SPE 3012 Presented at Journal of Petroleum Technology, December, 1971.

Slider, H. C. A simplified method of pressure buildup analysis for a stabilized well. Paper SPE 3335 Presented at Journal of Petroleum Technology, September, 1971.

Stakgold, I. Green's functions and boundary value problems. Academic Press Inc., San Diego, California, USA, 1998.

Stehfest, H. Numerical inversion of laplace transforms. Communications of Association for Computing Machinery, 1970, 13(1): 47-49.

Streltsova, T. D. Buildup analysis for interference tests in stratified formations. Paper SPE 10265 Presented at Journal of Petroleum Technology, February, 1984.

Theis, C. V. The relation between the lowering of the piezometric surface and the rate and duration of discharge of a well using ground-water storage. Eos, Transactions American Geophysical Union, 1935, 16(2): 519-524.

Tuma, J. J. Engineering mathematics handbook. New York City, USA, McGraw-Hill Professional, 1997.

Umnuayponwiwat, S., Ozkan, E. Pressure transient behavior and inflow performance of multiple wells in closed systems. Paper SPE 62988 Presented at the SPE Annual Technical Conference and Exhibition, Dallas, Texas, 1–4 October, 2000.

Uraiet, A. A., Raghavan, R. Pressure buildup analysis for a well produced at constant bottomhole pressure. Paper SPE 7984 Presented at Journal of Petroleum Technology, October, 1980.

Van Everdingen, A. F., Hurst, W. The application of the Laplace transformation to flow problems in reservoirs. Paper SPE 949305 Presented at Journal of Petroleum Technology, December, 1949.

Van Everdingen, A. F. The skin effect and its influence on the productive capacity of a well. Paper SPE 203 Presented at Journal of petroleum technology, June, 1953.

Zwillinger, D. Standard mathematical tables and formulae. New York City, USA, CRC Press Taylor and Francis Group, 1996.